Journal of Catalysis **207,** 256–265 (2002)
doi:10.1006/jcat.2002.3520, available online at http://www.idealibrary.com on IDEAL®

Characterization of Silica-Supported Molybdenum and Tungsten Phosphide Hydroprocessing Catalysts by ^{31}P Nuclear Magnetic Resonance Spectroscopy

P. Clark, X. Wang, and S. T. Oyama[1]

Environmental Catalysis and Materials Laboratory, Department of Chemical Engineering (0211), Virginia Polytechnic Institute and State University, Blacksburg, Virginia 24061

Received July 17, 2001; revised January 4, 2002; accepted January 4, 2002

Silica-supported molybdenum phosphide, MoP/SiO_2, and tungsten phosphide, WP/SiO_2, were prepared and characterized for their catalytic activity in hydrodenitrogenation (HDN) and hydrodesulfurization (HDS). The silica-supported phosphides were tested in the simultaneous hydroprocessing of quinoline and dibenzothiophene at 3.1 MPa and 643 K and were compared to a MoS_2/SiO_2 sample. The supported phosphides had superior HDN and lower HDS activity compared to the sulfide under these conditions. The conversion levels of MoP/SiO_2 were similar to those of bulk MoP, while the WP/SiO_2 was somewhat less active than its bulk WP counterpart. However, when compared on a CO uptake basis, the bulk materials had a clear performance advantage. Solid state nuclear magnetic resonance measurements indicated ^{31}P shifts from 85% H_3PO_4 of 255 ppm for WP and 214 ppm for MoP. Comparison of freshly prepared and passivated samples indicated that the supported phosphides were susceptible to surface oxidation on exposure to the atmosphere as a result of their small particle size. © 2002 Elsevier Science (USA)

Key Words: **hydrodenitrogenation; hydrodesulfurization; silica; tungsten phosphide; molybdenum phosphide; quinoline; dibenzothiophene; ^{31}P NMR.**

INTRODUCTION

Transition metal phosphides like MoP (1–3), WP (4), Ni_2P, and Co_2P (5, 6) constitute a new class of catalysts that have recently been reported to be active for hydroprocessing reactions. This is currently an important area, as there is a need to develop better catalysts to meet severe environmental restrictions on the content of sulfur in transportation fuels. Fundamental understanding of the differences between compounds like MoP and MoS_2 is needed in order to design improved materials. The objectives of the present investigation are to study the preparation of MoP and WP deposited on a silica support and to compare their performance to the unsupported catalysts. A further objective is to determine the applicability of ^{31}P magic-angle spinning–nuclear magnetic resonance (MAS–NMR) spectroscopy for the study of the bulk and supported phosphide samples. Except for one study in our group on WP (7), this technique has not been applied to transition metal phosphides and the spectra presented here are the first to be reported in the literature. The NMR measurements indicate that the silica-supported MoP and WP samples are susceptible to oxidation on exposure to the atmosphere. However, complementary X-ray diffraction measurements show that at reaction conditions the principal supported phases remain phosphides.

The use of silica for hydroprocessing catalysts has not been widely studied because weak interactions with the active phase generally lead to low dispersions (8). It is generally thought that the surface of the silica support contains coordinatively saturated bridging oxide species and surface hydroxyls but is essentially neutral in character (9). This is in contrast to the alumina surface which contains hydroxyl groups with amphoteric character (10) and which interacts strongly with metal (11, 12), sulfide (13), phosphate (14), and phosphide (15) adsorbents. It has been reported that silica-supported CoMo catalysts prepared by impregnation exhibit low hydrotreating activity compared to Al_2O_3-supported catalysts (16), and this has been attributed to the low dispersion of Co and Mo after calcination. However, it has been found that low loading (2–4 wt%) samples of MoS_2/SiO_2 can perform better than their Al_2O_3 counterparts (17, 18). In fact, silica-supported Co sulfide having 7.4% loading has been recently proposed as an inexpensive alternative to conventional catalysts (19). We have undertaken this study to investigate the suitability of SiO_2 as a support for MoP and WP.

EXPERIMENTAL

Catalyst Preparation and Characterization

Catalysts were prepared by incipient wetness impregnation of a silica support with aqueous metal phosphate

[1] To whom correspondence should be addressed. E-mail: oyama@vt.edu.

0021-9517/02 $35.00
© 2002 Elsevier Science (USA)
All rights reserved.

precursors, followed by temperature-programmed reduction (TPR) in flowing hydrogen. The silica support (Cabot, Cabosil L90, 99.8%) consisted of 0.2- to 0.3-μm aggregates of spherical particles ~30 nm in diameter prepared by vapor-phase hydrolysis of $SiCl_4$ in a H_2–O_2 flame (20). Stoichiometric amounts of ammonium paramolybdate, $(NH_4)_6Mo_7O_{24} \cdot 4H_2O$ (Aldrich, 99%), or ammonium metatungstate $(NH_4)_6W_{12}O_{39} \cdot xH_2O$ (Aldrich, 90%) were combined with ammonium phosphate $(NH_4)_2HPO_4$ (Aldrich, 99%) in distilled water, and the solution was used to impregnate the silica support by the incipient wetness technique. The concentration of Mo, W, and P in the solution was 0.73 mol/dm^3. The moist paste was calcined in air at 773 K for 6 h, ground and mixed, then pressed, broken, and sieved between 650- and 1180-μm screens to form pelletized supported phosphate materials. The molar loadings of molybdenum and tungsten monophosphide were held constant at 1.16 mmol each of Mo, W, and P per g of silica, leading to 13 wt% MoP/SiO_2 and 20 wt% WP/SiO_2. Sulfidation of samples containing 5.0 wt% MoO_3 and 13 wt% MoO_3 (0.37 and 1.16 mmol of MoO_3 per g of silica) led to 5.6 and 17 wt% MoS_2/SiO_2, respectively.

The precursor phosphates were loaded in quartz u-tube reactors and were reduced to phosphides using linear temperature ramps (0.0833 K s^{-1}, 5.0 K min^{-1}) in flowing hydrogen. Hydrogen flow was set at 650 μmol s^{-1} g^{-1} of starting material (e.g. 300 cm^3(NTP) min^{-1} H_2 flow for a 0.300-g sample) for all syntheses. The final temperature was 850 K for the MoP/SiO_2 and 1000 K for the WP/SiO_2, with this temperature held for 2 h to ensure completion of reaction. Species in the effluent were identified periodically (2–5 s) by a mass spectrometer (Dycor/Ametek MA100) to follow the progress of the reaction. Water was the only gaseous reaction product observed; no P_2 ($m/z = 62$) or PH_3 ($m/z = 34$) were detected. Occasionally, though, traces of a yellow insoluble deposit were formed downstream in the reactor following the higher temperature preparation of WP/SiO_2. After reduction, the phosphide was cooled to room temperature under 65 μmol s^{-1} of helium, and typically was passivated progressively by flowing 78 μmol s^{-1} of 0.1 mol% O_2/He overnight, followed by 13 μmol s^{-1} of 0.5 mol% O_2/He for 2 h. The reactor was then disconnected from the flow system, and ambient air was allowed to diffuse in for 24 h before collecting the sample from the tube.

Unsupported MoP and WP reference samples were also synthesized from phosphate precursors as reported earlier (1, 4). The bulk MoP was prepared by TPR to 913 K at 0.0833 K s^{-1} (5 K min^{-1}), and the bulk WP by TPR to 973 K at the same heating rate.

MoS_2/SiO_2 samples were prepared by sulfiding 5 wt% MoO_3/SiO_2 and 13 wt% MoO_3/SiO_2 for 2 h in a stream of 10 mol% H_2S/H_2 at 678 K, following a temperature ramp of 0.0833 K s^{-1} (5 K min^{-1}). The sulfide sample used for hydroprocessing was sulfided directly from the oxide within the catalytic reactor at a flow rate of 98 μmol s^{-1} (150 cm^3 of NTP min^{-1}) of 10% H_2S/H_2 at atmospheric pressure. The characterization of the sulfide samples by O_2 chemisorption also directly followed sulfidation of the oxide. For the chemisorption measurements on MoS_2/SiO_2, 0.3 g of oxide was sulfided in 195 μmol s^{-1} of 10% H_2S/H_2 employing the same temperature program used for the catalyst samples.

All gases were supplied by Air Products. Hydrogen, helium, and carbon monoxide were all 99.999% pure and were passed through a water trap (Alltech) before coming into contact with the sample. Specialty mixtures, including 0.5% O_2/He, 30% N_2/He, and 10% H_2S/H_2, were used as received.

The total dynamic CO uptakes of the phosphides were measured by passing pulses of CO (5.6 μmol) in a stream of 40 μmol s^{-1} of helium over 0.3-g samples at room temperature. Passivated samples were characterized after rereduction at 723 K in H_2. The phosphides used in all our studies were used within a month of preparation, as it was found that longer term storage in closed vials resulted in a slow degradation, probably due to oxidation. Uptakes of O_2 for the sulfides were measured in an identical manner at dry ice/acetone temperature (195 K). The O_2 uptakes were multiplied by a factor of 2 to account for dissociative adsorption on the surface. Surface area measurements were performed on air-exposed samples by N_2 adsorption using a Micromeritics 2000 sorption unit.

X-ray diffraction (XRD) spectra were collected with a Scintag XDS-2000 X-ray diffractometer using Ni-filtered Cu$K\alpha$ ($\lambda = 0.1541$ nm) radiation. Scans were collected at a rate of 0.035° 2θ s^{-1} and increments of 0.03° 2θ. Crystallite sizes were estimated from the diffraction patterns using the Scherrer equation, $D_{hkl} = K\lambda/\beta \cos\theta$. The constant K was taken here to be 0.9, and the average of the strongest two reflections was used to determine the reported values (21).

Nuclear Magnetic Resonance

Characterization of the samples by ^{31}P MAS–NMR was carried out using a Bruker (MSL 300) instrument operating at 300 MHz. A single-pulse method was used with a pulse delay of 3 μs, an acquisition delay of 3 ms, a recycle delay of 1 s, and approximately 14,500 acquisitions. Measurements were taken at different sample rotation (SR) speeds. Chemical shifts are referenced to 85% H_3PO_4. Samples were loaded into Kel-F capped zirconia rotors without exposure to the atmosphere in a glove box (*in situ*), or were passivated with 0.5% O_2/He and exposed to the atmosphere (*ex situ*).

Reactivity Testing

Hydroprocessing activity was measured by hydrotreatment of a model liquid containing quinoline and dibenzothiophene at 643 K (370°C) and 3.1 MPa (450 psig) in

TABLE 1

Composition of Model Oil

Component	mol%	wt%	N, S, O (wppm)	Delivery rate (μmol h^{-1})
Quinoline	2.6	1.9	2000	580
Dibenzothiophene	1.7	1.7	3000	380
Benzofuran	0.6	0.4	500	130
Tetralin	27	20	0	6,100
Tetradecane	68	76	0	15,500

TABLE 2

Compositional Characteristics of Silica-Supported Catalysts

Sample[a]	mmol of metal g^{-1} of SiO_2	Metal atom nm^{-2} of SiO_2
5.6% MoS_2/SiO_2	0.37	2.44
13% MoP/SiO_2	1.16	7.67
20% WP/SiO_2	1.16	7.67

[a] Weight percent MoP, WP, or MoS_2.

an upward-flow, fixed-bed reactor as described earlier (22). Compositional characteristics and delivery rates of the feed liquid are summarized in Table 1. With the exception of tetradecane of purity 99 mol% , which was purchased from Fisher, chemicals were obtained from Aldrich and had a purity level of 97+%.

To start a reaction, samples were placed in the catalytic reactor and pretreated before starting the oil delivery. The phosphide catalysts were pretreated in 100 μmol s^{-1} of hydrogen at 723 K and 1-atm pressure for 2 h. The sulfide catalyst was pretreated by sulfiding the oxide directly in the catalytic reactor, with a 10 mol% H_2S/H_2 mixture at 678 K and 1-atm pressure for 2 h. After the pretreatment, the reactor conditions were set to 3.1 MPa (450 psig), a hydrogen flow rate of 100 μmol s^{-1} (150 cm^3 NTP min^{-1}), a liquid feed rate of 0.0833 cm^3 s^{-1} (5 cm^3 min^{-1}), and 643 K. The amounts of catalysts used in this study were 2.6 g of MoS_2/SiO_2, 1.4 g of MoP/SiO_2, and 3.1 g of WP/SiO_2. These amounts corresponded to roughly similar quantities (70, 70, and 58 μmol, respectively) of chemisorption sites. For the SiO_2 blank, an arbitrary amount of 3 g was employed, as the material had negligible chemisorption of CO. The compositions of hydroprocessed liquid samples were identified with a Hewlett Packard 5890A gas chromatograph (equipped with a CP Sil 5B column) on samples collected at 2- to 3-h intervals. Reaction products were identified through matching of retention times with commercially available chemicals. Characterization of catalysts after reaction by XRD was made after washing the collected samples in *n*-hexane, drying in air, and mounting ~1-mm-thick powder films on top of a glass slide.

RESULTS

Preparation and Characterization

Silica-supported molybdenum phosphide, tungsten phosphide, and molybdenum sulfide catalysts were prepared by incipient wetness impregnation of a silica support with ammonium salts of Mo, W, and P dissolved in distilled water. Compositional characteristics of each sample are summarized in Table 2.

Oxidic catalyst precursors were reduced to phosphide form by temperature-programmed reduction in hydrogen and were subsequently passivated. Prior to the reactivity measurements and *ex situ* CO uptake characterization, passivated phosphides were pretreated in hydrogen at 723 K for 2 h to remove the surface oxide layer.

The temperature-programmed reduction (TPR) trace at 5 K min^{-1} of MoP/SiO_2 is compared to that of bulk MoP in Fig. 1. The predominant reduction features appeared at 680 and 820 K for the supported sample and 770 and 920 K for the unsupported reference. X-ray diffraction (XRD) patterns of the fresh and spent MoP/SiO_2 samples are shown in Fig. 2 along with that of a bulk MoP reference. An insert depicts the crystal structure of MoP. The diffraction patterns of the supported catalysts showed only features of bulk MoP and amorphous silica (the broad peak near 22° 2θ) both before and after reaction.

The TPR traces of WP/SiO_2 and WP are shown in Fig. 3. Here, the predominant reduction peaks occurred at 890 and 970 K for the supported material and 1010 K for the unsupported reference. XRD patterns of the fresh and spent WP/SiO_2 samples are shown in Fig. 4 along with that of a bulk WP reference. Again the insert depicts the crystal structure. The diffraction patterns of the supported catalyst showed features only of WP and amorphous silica both before and after reaction in hydrotreating.

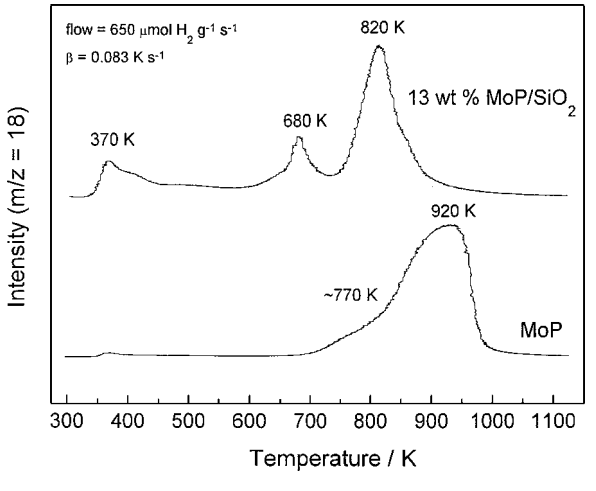

FIG. 1. Temperature-programmed reduction profiles in the preparation of MoP/SiO_2 and MoP at 0.0833 K s^{-1} (5 K min^{-1}).

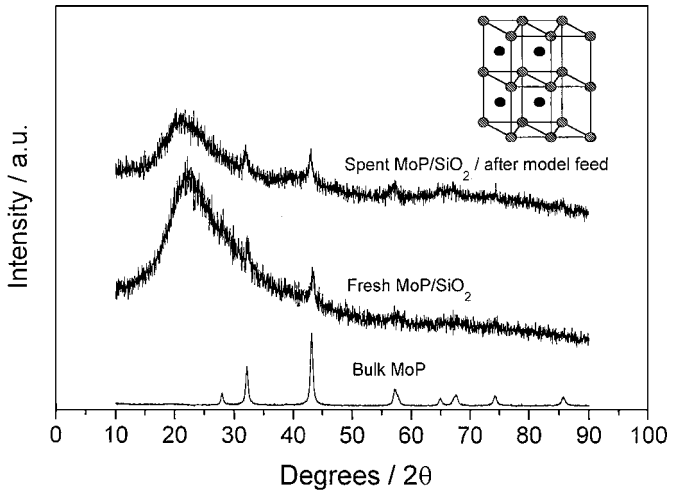

FIG. 2. X-ray diffraction spectra for fresh and spent MoP/SiO$_2$ samples.

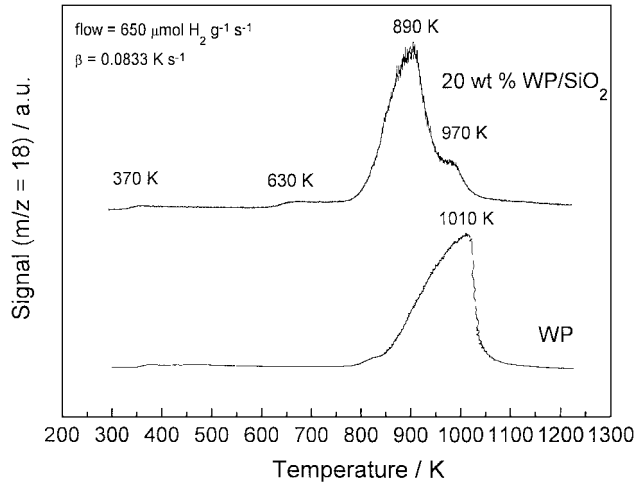

FIG. 3. Temperature-programmed reduction profiles in the preparation of WP/SiO$_2$ and WP at 0.0833 K s^{-1} (5 K min^{-1}).

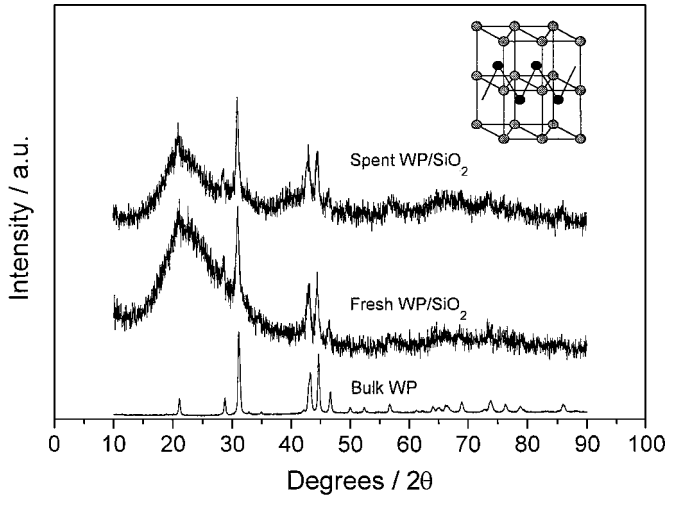

FIG. 4. X-ray diffraction spectra for fresh and spent WP/SiO$_2$ samples.

TABLE 3

Physical Characteristics of Silica-Supported Catalysts

Sample	Surface area[a] ($m^2\ g^{-1}$)	Crystallite size[a] (nm)	CO uptake[b] Fresh	CO uptake[b] Spent	Surface metal sites[c]	Dispersion[d] (%)
SiO_2 blank	91	—	0	0	—	—
5.6% MoS_2/SiO_2	93	—	27[e]	—	—	5.2
17% MoS_2/SiO_2	—	—	7[e]	—	—	0.7
13% MoP/SiO_2	50	15[f]	50	26	110	4.9
20% WP/SiO_2	62	16[g]	19	6.5	94	2.0
MoP	8	18[f]	15	4.5	130	0.2
WP	10	23[g]	10	11	140	0.2

[a] Passivated catalysts.
[b] CO uptake at 298 K in μmol g^{-1}; sample pretreated at 723 K in H_2.
[c] Calculated in μmol g^{-1} from formula in text.
[d] CO uptake (fresh)/mol of metal.
[e] O_2 uptake at 78 K; sample presulfided at 678 K in 10% H_2S/H_2.
[f] Average of (100) and (101) directions.
[g] Average of (101) and (002) directions.

The chemisorption and surface area properties of the catalysts are summarized in Table 3. The incorporation of phosphides onto the silica reduced the surface areas of the samples in both cases. The surface area of the sulfide was unaffected, presumably because of its low metal loading and low preparation temperature. The experimental CO uptakes dropped during the catalytic test.

Crystallite sizes, theoretical CO uptakes, and dispersions were calculated for MoP and WP catalysts based on their crystallite size, density, and loading. These values are also reported in Table 3. The calculation of crystallite sizes (D_{hkl}) with the Scherrer equation was described earlier, in the experimental section. Table 3 also reports the theoretical number of surface metal sites (μmol g^{-1}), assuming that the samples are composed of uniform spherical particles. It was calculated from

$$\text{Surface sites} = S_g \cdot \bar{n} \cdot f, \qquad [1]$$

where S_g is the specific surface area ($m^2\ g^{-1}$) either measured (for the bulk samples) or calculated (for the supported samples) from the crystallite size and density by the equation

$$S_g = \frac{6}{D_{hkl} \cdot \rho}. \qquad [2]$$

The quantity $\bar{n}$ is the areal density, the number of metal atoms per unit surface, and f is the fractional weight loading (g of MoP/g of catalyst or g of WP/g of catalyst) of the sample. The areal density is taken here to be 16.1 μmol m^{-2} for MoP, as calculated from the value of the surface area per metal atom of 10.3 Å^2, as reported previously (2). The corresponding values for WP were derived from its crystal structure to be 14.5 μmol m^{-2} and 11.6 Å^2 atom^{-1}.The density, ρ, was taken to be 7.50 g cm^{-3} for MoP and 12.4 g cm^{-3} for WP (23). The crystallite sizes of the phosphides

supported on silica were smaller than the crystallite sizes of the bulk material.

Dispersions were calculated from the fresh chemisorption uptakes, assuming a stoichiometry of 1 CO per surface metal atom. These values are also reported in Table 3. The dispersions were generally low, indicating poor distribution of the components on the support. This is typical of the behavior of metallic compounds on silica supports.

Nuclear Magnetic Resonance Spectroscopy

Characterization of the catalysts by ^{31}P MAS–NMR was carried out on both fresh (*in situ*) and passivated (*ex situ*) samples. Figure 5 shows the NMR spectra of the bulk WP at different sample rotation (SR) speeds. The *in situ* spectra (Fig. 5a) displayed a complex pattern in which the positions of only two peaks, at 255 and −6 ppm (arrows), were invariant with rotation. The *ex situ* spectra (Fig. 5b) again showed a number of peaks, with the same ones remaining invariant, but with the intensity pattern changed considerably, and with the peak at low field becoming dominant and slightly shifted to −3 ppm. Figure 6 shows similar NMR results for the WP/SiO_2 sample. Again, the *in situ* sample (Fig. 6a) had two peaks that were invariant with rotation at 254 and −5 ppm (arrows), while the *ex situ* sample (Fig. 6b) had an altered pattern with the peak at low field becoming dominant and slightly shifted to −3 ppm. Table 4 gives a summary of the observed chemical shifts.

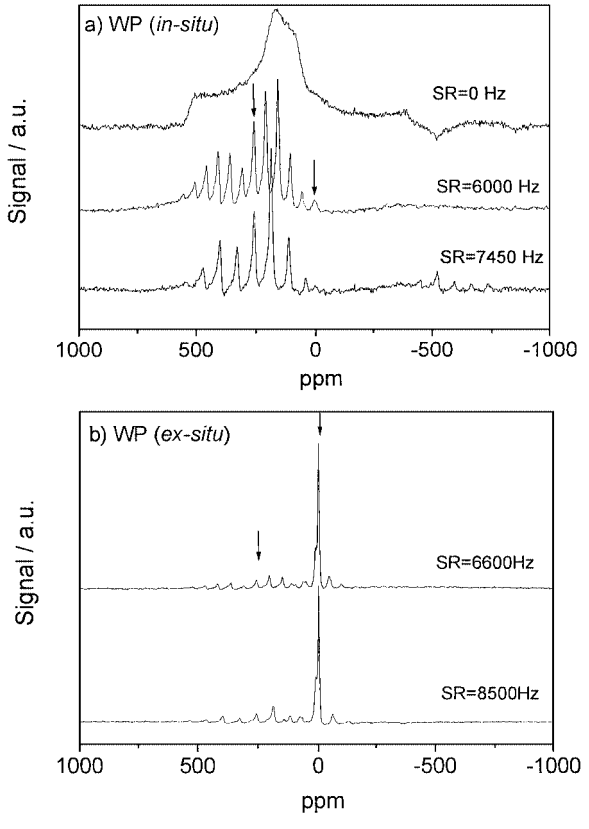

FIG. 5. ^{31}P MAS–NMR spectra: (a) WP *in situ*, (b) WP *ex situ*.

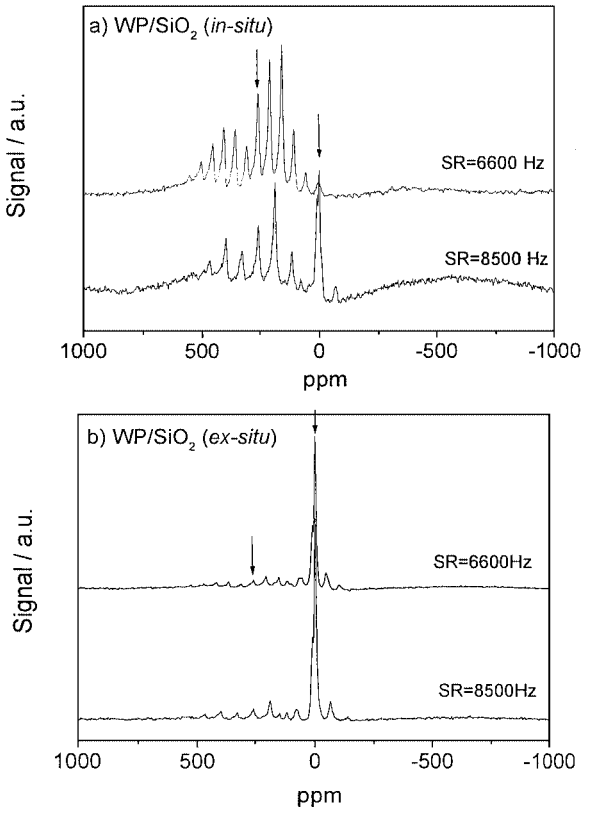

FIG. 6. ^{31}P MAS–NMR spectra: (a) WP/SiO_2 *in situ*, (b) WP/SiO_2 *ex situ*.

Figure 7 shows the NMR spectra of the unsupported MoP sample at *in situ* and *ex situ* conditions. The *in situ* spectrum (Fig. 7a) displayed a complex pattern that was completely different from that of the bulk WP sample, but which again had two peaks, at 214 and −5 ppm (arrows), that did not shift with sample rotation. The *ex situ* sample (Fig. 7b) showed a similar pattern but the signals were much noisier and were overlaid on a sinusoidal baseline. Again, two invariant peaks were observed, with the low-field peak enhanced and shifted to −3 ppm. Figure 8 shows the results for the MoP/SiO_2 sample. The *in situ* spectra (Fig. 8a) displayed considerable noise and an uneven baseline, with weak and unresolved features at 199 and −36 ppm (arrows). The *ex situ* spectra (Fig. 8b) were completely dominated by the low-field feature at −5 ppm, with the high-field peaks barely discernible.

Reactivity

The progress of the hydroprocessing reactions of dibenzothiophene and quinoline at 643 K and 3.1 MPa using MoP/SiO_2 and WP/SiO_2 are shown in Fig. 9. Both materials reached stable conversion levels after only 20 h of reaction.

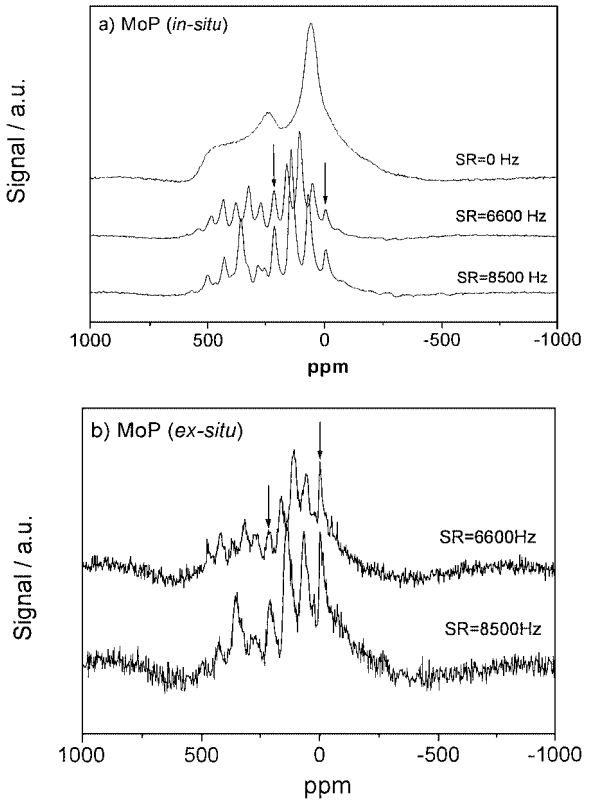

FIG. 7. ^{31}P MAS–NMR spectra: (a) MoP *in situ*, (b) MoP *ex situ*.

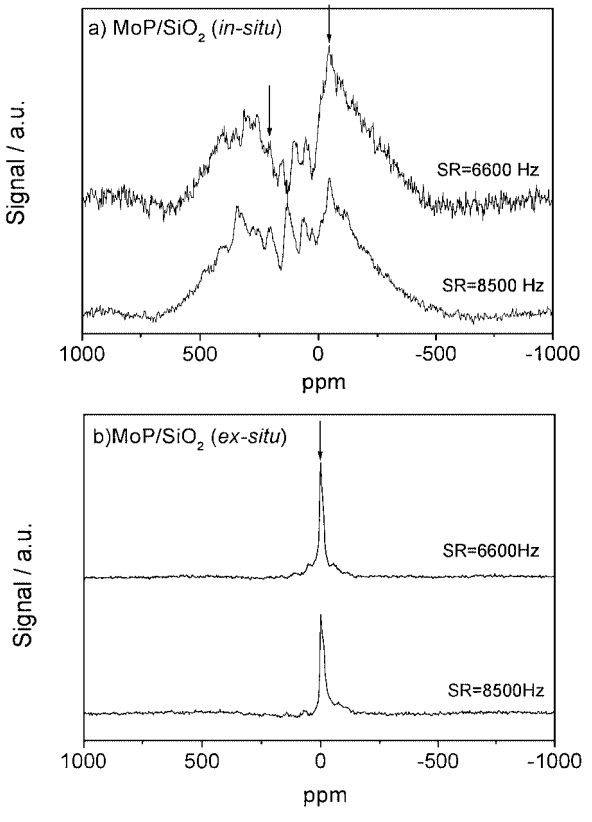

FIG. 8. ^{31}P MAS–NMR spectra: (a) MoP/SiO_2 *in situ*, (b) MoP/SiO_2 *ex situ*.

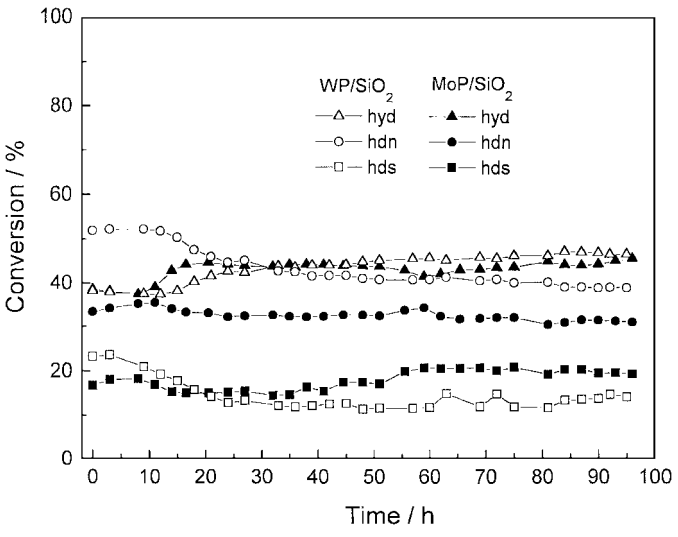

FIG. 9. Time dependence of the hydroprocessing activity of MoP/SiO_2 and WP/SiO_2 catalysts in the conversion of a model feed at 643 K and 3.1 MPa.

DISCUSSION

Preparation and Characterization

The reduction profile obtained in the preparation of the MoP/SiO_2 catalyst is presented in Fig. 1 and is compared to the reduction profile of bulk MoP taken under similar conditions. The reduction trace of MoP/SiO_2 showed a feature at low temperature (370 K) and two peaks at high temperatures (680 and 820 K). The low-temperature feature was due to the dehydration of the sample, while the high-temperature peaks were indicative of the reduction stages of the phosphate. XRD analysis of the intermediate stage indicated that the first high-temperature peak, at 680 K, was due to the initial stages of reduction of Mo to a lower oxidation state, while the second peak, at 820 K, was associated with the further reduction of both phosphorus and molybdenum to form MoP. These results will be presented in a separate, more detailed study of the preparation (24). It can be seen that the synthesis reaction was substantially over at 850 K and this was used as the final reduction temperature for the preparation of the MoP/SiO_2 catalyst. A holding time of 2 h was used at this temperature to ensure completion of the reduction.

The bulk MoP reduction profile was obtained at the same heating rate of 0.0833 K s^{-1} (5 K min^{-1}) as the supported sample and also showed two high-temperature reduction processes. However, the first peak was unresolved and both peaks were shifted to higher temperatures (770 and 920 K). This was likely due to the presence of larger particles reacting in a shell-to-core manner and inhibition of reaction by water formed by the reaction (25).

The TPR traces (Fig. 1) of the molybdenum phosphide samples can be analyzed to obtain the average rate of formation of the product phosphide, and hence the rate of

consumption of hydrogen. From the temperature program and duration of the main reduction peaks (full width at half maximum = 65 K) it is possible to extract the time of reaction (800 s). This information, combined with knowledge of the total amount of sample in the preparation, yields the average rate of hydrogen consumption. Assuming that the stoichiometry of the supported material is similar to that of the bulk, as determined gravimetrically, $MoPO_{5.5} + 5.5H_2 \rightarrow MoP + 5.5H_2O$, the rate of hydrogen consumption for the supported sample can be calculated to be 6.9 μmol g^{-1} s^{-1}. This compares to the flow rate of hydrogen of 650 μmol g^{-1} s^{-1}, which is a factor of 94 times larger. Therefore, the reaction is unlikely to be inhibited by the water produced by the reaction.

For the unsupported sample (full width at half maximum = 120 K, or 1500 s) the corresponding rate of hydrogen consumption is 28 μmol g^{-1} s^{-1}. The flow rate of hydrogen is now only 24 times larger, and the possibility of product inhibition by the water formed in the reaction is larger.

Another effect which is also likely to be contributing to the retardation of the reduction peaks in the bulk material is shell-to-core reduction. The average particle size of the bulk starting material can be calculated using the expression diameter = 6/surface area · density (where surface area = 1.3 m^2 g^{-1}, $\rho = 3.54$ cm^3 g^{-1}) to be 1.3 μm. This was likely to be much larger than the particle size of the supported phosphate precursor. Since the rate of reaction in the shrinking-core model depends on the square of the particle size (26, 27), this probably also contributed to the observed shift in the temperature of reaction between the bulk and silica-supported materials.

Assuming the stoichiometry of bulk reduction indicated above the final stoichiometry of the phosphides is MoP and WP. As is discussed below this is supported by the XRD and NMR results. These compounds have a metallic nature (28), so it is expected that the oxidation states of Mo and W will be close to zero. However, it is likely that some charge transfer will occur to the electronegative P atoms, so in fact the Mo and W should be slightly oxidized.

The XRD spectra of the bulk MoP and supported MoP samples prepared at 850 K, before and after the hydrotreating reactions, are shown in Fig. 2. The bulk MoP had a pattern which corresponded exactly to that reported in the literature (powder diffraction file 24-771). MoP has a hexagonal WC-type structure (strukturbericht designation, B_h) with space group $P_{\bar{6}m2}$ and lattice parameters $a_0 = 322$ pm and $c_0 = 319$ pm (29). The insert shows a schematic of the structure, which is based on a stacked arrangement of trigonal prisms. The supported MoP/SiO_2 showed a broad feature at $\sim 22^\circ$ 2θ produced by the amorphous silica support, and several distinct peaks which matched those of the bulk MoP phase.

The reduction profile for the preparation of WP/SiO_2 catalyst is presented in Fig. 3 and is compared to the reduction profile for bulk WP collected under similar conditions. The reduction trace of WP/SiO_2 showed a small feature at 370 K, a slight rise at 630 K, and a large peak at 890 K with a high-temperature shoulder at 970 K. The feature at 370 K was due to dehydration of the sample, while the high-temperature peaks were due to formation of phosphide. The slight rise at 630 K may have been due to small quantities of highly dispersed species, while the shoulder at high temperature may have arisen from larger particles which reduced more like the bulk WP. It is clear from the figure that the reduction process was essentially completed at 1000 K, which was used as the maximum temperature in the preparation of the WP catalyst. Again, a hold time of 2 h was used to ensure complete reduction of the sample.

The reduction profile of the bulk WP also showed the slight dehydration feature at 370 K and a high-temperature reduction peak at 1010 K. Similarly to the case of supported and unsupported MoP, the largest peak was shifted to higher temperature, likely as a result of the inhibitive action of water vapor and the presence of larger particles in the bulk material.

The XRD spectra of the bulk WP and supported WP samples prepared at 1000 K, before and after hydrotreating reactions, are shown in Fig. 4. The bulk WP had a pattern corresponding exactly to that reported in the literature (powder diffraction file 29-1364). WP adopts the orthorhombic MnP type structure (strukturbericht designation, B_{31}) with space group P_{nma} and lattice parameters $a_0 = 571$ pm, $b_0 = 325$ pm, and $c_0 = 623$ pm (30). The insert shows a schematic of the structure, which like MoP is based on a stacked arrangement of trigonal prisms. However, in WP the second row is displaced laterally half a lattice spacing and the phosphorus atoms are linked in chains. The supported WP/SiO_2 showed a broad feature at $\sim 22^\circ$ 2θ due to the silica support, and several distinct peaks which matched those of the WP phase.

The *ex situ* chemisorption characteristics and BET surface areas of catalyst samples are summarized in Table 3. The surface area of the MoS_2/SiO_2 catalyst (93 m^2 g^{-1}) precursor was close to that of the support (91 m^2 g^{-1}), as its loading was low. The surface areas of the MoP/SiO_2 (50 m^2 g^{-1}) and WP/SiO_2 (62 m^2 g^{-1}) samples were significantly decreased from that of the support. This is a common finding for phosphorus-promoted, supported catalysts (31, 32), and probably occurs as a result of solid state reactions or pore clogging promoted by phosphorus compounds. In the case of the phosphides studied here, the use of elevated temperatures during sample reduction, 850 K for MoP/SiO_2 and 1000 K for WP/SiO_2, may have contributed to the decrease in surface area by sintering of the silica support. Chemisorption quantities of O_2 and CO for the fresh catalysts were moderate and were found to decrease somewhat after reaction for the phosphides. Measurements taken after reaction were carried out on recovered samples washed in

hexane and re-reduced at 723 K for 2 h. The CO uptakes of MoP/SiO_2 and WP/SiO_2 and O_2 uptake of MoS_2/SiO_2 were used to calculate dispersions based on stoichiometries for adsorption of one CO molecule and one O atom per surface metal atom. The dispersions are reported in Table 3. They were low, 5.2% for 5.6% MoS_2/SiO_2, 0.7% for 17% MoS_2/SiO_2, 4.9% for MoP/SiO_2, and 2.0% for WP/SiO_2, consistent with the observation of crystalline phases for the phosphides.

The very low dispersion of the 17% MoS_2/SiO_2 was probably due to the formation of large domains exposing inactive basal planes. For this reason the low-loading 5.6% MoS_2/SiO_2 sample was used for the reactivity measurements.

The crystallite sizes of the phosphide samples were determined by Scherrer analysis and are reported in Table 3. As indicated in the table, the crystallite sizes were taken as averages over two principal directions. Although not shown, the crystallite dimensions in those directions were not substantially different (<5%), indicating that the particle morphology was globular.

The crystallite sizes can be used to calculate the theoretical number of surface metal sites (μmol g^{-1}) based on clean surfaces and spherical particles, and these are also reported in Table 3. For the unsupported materials the number of surface sites were considerably larger than the CO uptakes, indicating that a large proportion of the surface (89% for MoP, 93% for WP) was unable to chemisorb CO. This may have been due to site blockage by phosphorus or strongly held oxygen. For the supported samples the number of sites was closer to the actual uptakes, indicating that a smaller proportion of their surfaces was blocked (55% for MoP/SiO_2, 80% for WP/SiO_2).

Nuclear Magnetic Resonance

The ^{31}P MAS–NMR spectra (Figs. 5–8) are the first reported for supported metallic phosphides in the literature. The spectrum of the bulk WP (Fig. 5a) at zero rotation showed an asymmetric envelope characteristic of considerable electric-field anisotropy surrounding the phosphorus nucleus. This can be understood from the crystal structure (Fig. 4), which shows that the phosphorus atoms reside in sites which look different, when approached from the x, y, or z directions. When the samples were rotated, the anisotropy was folded over to the spinning side bands, resulting in a complex intensity pattern. Nevertheless, crystallographically all the phosphorus atoms were equivalent, and the position of only one major peak, at 255 ppm, was invariant with rotation. A smaller peak at −6 ppm was due to a small amount of phosphate impurity. Chemical shifts in this range are typical for phosphates (14). For the passivated WP sample (Fig. 5b) this peak shifted to −3 ppm and became the dominant feature of the spectrum. The passivation procedure for the NMR samples was less gentle (0.5% O_2/He followed by air exposure) than for the catalysts (gradual increase in O_2 concentration) and probably resulted in more oxidation. There is also the likelihood that the intensity of the insulator phosphate signal is intrinsically stronger than that of the metallic phosphide, where the phosphorus is surrounded by conduction electrons.

TABLE 4

Summary of Chemical Shifts for Phosphide Catalysts[a]

Sample	Phosphide (ppm)		Phosphate (ppm)	
	In situ	Passivated	*In situ*	Passivated
WP	255	254	−6	−3
WP/SiO_2	254	254	−5	−3
MoP	214	214	−5	−3
MoP/SiO_2	199	None	−36	−5

[a] Reference: 85% H_3PO_4.

The spectra of the supported WP/SiO_2 samples (Fig. 6) show features very similar to the bulk references (Fig. 5). The *in situ* pattern (Fig. 6a) indicated a larger amount of phosphate than in the bulk reference. This was likely due to the smaller crystallite size in the supported materials (Table 3), which resulted in easier oxidation. In passivated samples the phosphate peak dominated the pattern (Fig. 6b), but the phosphide signature was clearly present. XRD analysis of this sample (Fig. 4) indicated the presence of crystalline WP, supporting the contention that the phosphate NMR signal is intrinsically strong compared to the phosphide, and not a good indicator of the real amounts of each phase. All the chemical shifts are summarized in Table 4. There are small shifts in the lines, but all can be readily assigned to phosphate or phosphide compounds.

The spectrum of the bulk MoP at zero rotation (Fig. 7a) also showed an asymmetric envelope, but different from that of WP. This is because MoP has a different structure (Fig. 2) than WP, but still has considerable anisotropy surrounding the phosphorus atoms. Rotation of the sample again produced a complex pattern of spinning side bands caused by the anisotropy, but one main peak, at 214 ppm, remained invariant. A second smaller peak, at −5 ppm, was due to the presence of some phosphate contaminant. Again, as with WP it is expected that the intensity of this phosphate peak is much stronger than that of the metallic phosphide signal, so the relative size of the peaks is not indicative of the amounts of each substance. When the sample was exposed to air (Fig. 7b) the phosphate peak shifted slightly, to −3 ppm, and grew in intensity. The noise level also went up substantially. For the case of the supported MoP/SiO_2 at *in situ* conditions (Fig. 8a) the noise level was also large, and the peaks for the phosphide and phosphate were barely discernible. In the case of the passivated sample (Fig. 8b) the phosphate signal completely

dominated the spectrum. It is likely that the MoP/SiO_2 is more easily oxidizable than the WP/SiO_2. Again, a summary of chemical shifts is given in Table 4. In conclusion, for both WP and MoP the NMR spectra showed that supporting the materials on SiO_2 allowed retention of the phosphide phases. Passivation of the samples resulted in some oxidation, with a greater severity for the MoP system.

Reactivity

The activity of the catalysts in the hydrodesulfurization (HDS) of dibenzothiophene and the hydrodenitrogenation (HDN) of quinoline was evaluated in a three-phase flow reactor at 643 K and 3.1 MPa. Figure 9 shows the conversions as a function of time on the silica-supported MoP and WP in HDS and HDN. Both materials demonstrated good stability in their activity levels. It should be noted that those results were obtained with 58 μmol of sites of WP/SiO_2 and 70 μmol of sites of MoP/SiO_2 loaded in the reactor. The conversions were corrected to equal sites assuming a first-order kinetic expression. Denoting X_1 as the conversion corresponding to a quantity of sites S_1, and X_2 as the conversion corresponding to S_2 sites, then the quantities are related by

$$\ln(1 - X_2) = \left(\frac{S_2}{S_1}\right) \cdot \ln(1 - X_1).$$

The results, corrected to 70 μmol of sites, for the supported MoP/SiO_2, WP/SiO_2, and MoS_2/SiO_2 are summarized in Table 5, along with results from bulk MoP and WP and the silica support. The conversion levels of MoP/SiO_2 were similar to those of the bulk MoP (1). However, adjustment by the CO uptake made the bulk appear better. This was a consequence of the low CO uptakes of the bulk material compared to the supported sample. Because of the low surface area of the bulk MoP, a strong possibility exists that a large fraction of the active surface is underestimated. The WP/SiO_2 sample differed most substantially from its unsupported counterpart (4) by having lower HDS activity. Again, this was due to the low CO uptake of the bulk material. Compared to the MoS_2/SiO_2 both phosphides had significantly higher HDN, but lower HDS.

TABLE 5

Summary of Hydroprocessing of Model Feedstock at 643 K and 3.1 MPa

Sample[a]	HDN[b] (%)	HYD[c] (%)	HDS[d] (%)
SiO_2	2	32	1
5.6% MoS_2/SiO_2	11	45	31
13% MoP/SiO_2	31	45	20
20% WP/SiO_2[e]	46	46	16
MoP[e]	54	34	24
WP[e]	88	33	92

[a] Reactor catalyst loading was 70 μmol of sites except for WP/SiO_2 (58 μmol) and bulk samples (30 m^2).

[b] Hydrodenitrogenation of quinoline.

[c] Hydrogenation of quinoline to N-containing products.

[d] Hydrodesulfurization of dibenzothiophene.

[e] Percentage of HDN and HDS adjusted to 70 μmol of sites according to first-order equation given in text.

The low apparent activity of the supported phosphides compared to the bulk references was surprising. It may have been that passivation resulted in overoxidation of the catalysts, as shown by NMR. Re-reduction of the catalysts produced the phosphides again, but perhaps in a different, less-active form from the bulk phosphides. This form may have had phosphides that were phosphorus deficient because of segregation. Nevertheless, the samples were completely stable to reaction conditions, as clearly shown by the XRD patterns after reaction (Figs. 2, 4).

In recent work (3) the group of Prins studied the HDN on a series of bulk phosphides at conditions similar to those employed in this work (3.0 MPa and 643 K). In the presence of sulfur they found HDN conversions of 10% for MoP and 30% for WP, which are somewhat lower than those found in this study, 31 and 46%, respectively. The comparison is not exact because the previous work used *o*-propylaniline instead of quinoline, bulk catalysts instead of supported catalysts, and slightly different catalyst weights. Considering these differences the results are comparable.

An interesting conclusion of this study is that sample morphology is important, especially in the case of a weakly interacting support like silica. In the case of molybdenum sulfide the effect of loading showed that low concentrations were required to produce samples of sufficient active surface. This can be understood from the layered structure of MoS_2, which has inactive basal planes and active edge planes. As the size of the crystallites grow with loading, they do so at the expense of the desirable side planes. However, for molybdenum and tungsten phosphide, which do not have a layered structure, the smaller interaction with silica probably produces particles of a globular morphology whose site density is much higher. This represents a special opportunity for these new materials, which could be exploited by the use of better supports than the silica used in this study.

CONCLUSIONS

MoP and WP were prepared on a silica support. They were moderately active catalysts for the hydrodenitrogenation of quinoline and the hydrodesulfurization of dibenzothiophene in a complex mixture. The silica-supported catalysts had similar temperature-programmed reaction profiles as those of the bulk samples, while having reduced hydroprocessing activities compared to the bulk materials. The smaller activity was partly due to the inaccuracy of

counting sites by CO chemisorption on the low-surface-area bulk materials. It could also have been the result of oxidation of the small particles of the phosphide on the support on exposure to air. A low loading was required to generate a MoS_2/SiO_2 samples of sufficient O_2 uptake for catalytic testing.

The materials were characterized using ^{31}P magic-angle spinning–nuclear magnetic resonance spectroscopy. WP and MoP gave isotropic signals shifted 255 and 214 ppm from 85% H_3PO_4, respectively. The presence of oxide was indicated by signals between −3 and −6 ppm whose intensity increased substantially with passivation.

ACKNOWLEDGMENTS

We appreciate the United States Department of Energy for funding this project through Grant DE-FG02-96ER14669. We also appreciate the surface area measurements provided by Doohwan Lee, and the assistance of Geno Iannaccone and Thomas Glass with the NMR measurements.

REFERENCES

1. Li, W., Dhandapani, B., and Oyama, S. T., *Chem. Lett.* 207 (1998).
2. Stinner, C., Prins, R., and Weber, T., *J. Catal.* **191**, 438 (2000).
3. Stinner, C., Prins, R., and Weber, Th., *J. Catal.* **202**, 187 (2001).
4. Clark, P., Li, W., and Oyama, S. T., *J. Catal.* **200**, 140 (2001).
5. Robinson, W. R. A. M., van Gastel, J. N. M., Korányi, T. I., Eijsbouts, S., van Veen, J. A. R., and de Beer, V. H. J., *J. Catal.* **161**, 539 (1996).
6. Wang, X., Clark, P., and Oyama, S. T., *J. Catal.*, in press.
7. Oyama, S. T., Clark, P., Wang, X., Shido, T., Iwasawa, Y., Hayashi, S., Ramallo-López, J. M., and Requejo, F. G., *J. Phys. Chem. B* **106**, 1913 (2002).
8. Breysse, M., Portefaix, J. L., and Vrinat, M., *Catal. Today* **10**, 489 (1991).
9. Iler, R. K., "The Chemistry of Silica: Polymerization, Colloid and Surface Chemistry and Biochemistry." Wiley, New York, 1979.
10. van Veen, J. A. R., Hendriks, P. A. J. M., Andréa, R. R., Romers, E. J. G. M., and Wilson, A. E., *J. Phys. Chem.* **94**, 5282 (1990).
11. Bartholomew, C. H., and Farrauto, R. J., *J. Catal.* **45**, 41 (1976).
12. Scheffer, B., Heijeinga, J. J., and Moulijn, J. A., *J. Phys. Chem.* **91**, 4752 (1987).
13. Reinhoudt, H. R., Crezee, E., van Langeveld, A. D., Kooyman, P. J., van Veen, J. A. R., and Moulijn, J. A., *J. Catal.* **196**, 315 (2000).
14. Iwamoto, R., and Grimblot, J., *Adv. Catal.* **44**, 417 (1999).
15. Oyama, S. T., Clark, P., Teixeira da Silva, V. L. S., Lede, E. J., and Requejo, F. G., *J. Phys. Chem. B* **105**, 4961 (2000).
16. van Veen, J. A. R., Gerkema, E., van der Kraan, A. M., and Knoester, A., *J. Chem. Soc. Chem. Commun.* **22**, 1684 (1987).
17. Luck, F., *Bull. Soc. Chim. Belges* **100**(11–12), 781 (1991).
18. Marzari, J. A., Rajagopal, S., and Miranda, R., *J. Catal.* **156**, 255 (1995).
19. Kogan, V. M., and Parfenova, N. M., *Stud. Surf. Sci. Catal.* **106**, 449 (1997).
20. "Cab-o-sil® Untreated Fumed Silica Properties and Functions." Cabot Corporation, Tuscola, IL, 1993.
21. Cullity, B. D., "Elements of X-ray Diffraction," 2nd ed. Addison–Wesley, Menlo Park, CA, 1978.
22. Ramanathan, S., and Oyama, S. T., *J. Phys. Chem.* **99**(44), 16365 (1995).
23. Schönberg, N., *Acta Chem. Scand.* **8**, 226 (1954).
24. Clark, P., and Oyama, S. T., manuscript in preparation.
25. Oyama, S. T., Schlatter, J. C., Metcalf, J. E., III, and Lambert, J. M., Jr., *Ind. Eng. Chem. Res.* **27**, 1648 (1988).
26. Lemaitre, J. L., *in* "Characterization of Heterogeneous Catalysts" (F. Delany, Ed.), p. 21. Dekker, New York, 1984.
27. Bathia, S., Beltramini, J., and Do, D. D., *Catal. Today* **7**(3), 309 (1990).
28. Aronsson, B., Lundström, T., and Rundqvist, S., "Borides, Silicides, and Phosphides." Methuen, London/Wiley, New York, 1965.
29. Rundqvist, S., and Lundstrom, T., *Acta Chem. Scand.* **17**, 37 (1963).
30. Rundqvist, S., *Acta Chem. Scand.* **16**(2), 287 (1962).
31. Kraus, H., and Prins, R., *J. Catal.* **170**, 20 (1997).
32. Lopez Cordero, R., Esquivel, N., Lazaro, J., Fierro, J. L. G., and Lopez Agudo, A., *Appl. Catal.* **48**, 341 (1989).